

## Research Article

# Spatiotemporal Relationship between Ecosystem Service Value and Ecological Risk in Disaster-Prone Mountainous Areas: Taking the Upper Reaches of the Minjiang River as an Example

Linsen Duan <sup>1</sup>, Huaiyong Shao <sup>1,2</sup>, Mingshun Xiang <sup>2,3</sup>, Hao Wang <sup>4</sup>,  
Chunjian Wang <sup>2,3</sup>, Hao Mei <sup>3</sup>, Yuxiang Tan <sup>3</sup> and Xiaofeng Yang <sup>3</sup>

<sup>1</sup>College of Earth Science, Chengdu University of Technology, Chengdu 610059, China

<sup>2</sup>Research Center for Human Geography of Tibetan Plateau and Its Eastern Slope, Chengdu University of Technology, Chengdu 610059, China

<sup>3</sup>College of Tourism and Urban-Rural Planning, Chengdu University of Technology, Chengdu 610059, China

<sup>4</sup>Piesat Information Technology Co., Ltd, Beijing 100195, China

Correspondence should be addressed to Huaiyong Shao; [shaohuaiyong@cdut.edu.cn](mailto:shaohuaiyong@cdut.edu.cn)

Received 2 August 2022; Revised 29 August 2022; Accepted 20 September 2022; Published 7 October 2022

Academic Editor: Zheng Liu

Copyright © 2022 Linsen Duan et al. This is an open access article distributed under the Creative Commons Attribution License, which permits unrestricted use, distribution, and reproduction in any medium, provided the original work is properly cited.

Mountainous areas are susceptible to disasters; the frequent occurrence of disasters drives the changes in ecosystem service value (ESV) and also brings certain ecological risk, which further increases the incidence of disasters. However, few scholars have investigated the spatiotemporal correlation between the ESV of disaster-prone mountainous areas and ecological risk index (ERI) with basin as the unit. This paper aims to clarify the spatial relationship between ESV and ERI under the changes of land use. Taking the upper reaches of the Minjiang River as the study area, the authors collected the land use data of 2000–2020, estimated ESV by the value equivalent factor per unit area method, and constructed the ERI. On this basis, the relationship between ESV and ERI was investigated in details. The results show the following: (1) From 2000 to 2020, the total ESV exhibited a fluctuating upward trend. The spatial distribution of ESV was greatly affected by slope and altitude; an important reason for the rising ESV in the study area is the increase of forest area and water area. (2) The upper reaches of the Minjiang River had a generally low ERI and relatively good overall ecoenvironment. After 2010, however, the ecological risk continued to rise. Most of the strongly high risk areas are areas with frequent human activities, such as low-altitude areas and river banks. (3) There is a spatial correlation and coupling between ESV and ERI in the study area; i.e., the strongly high ESV areas generally had a low ecological risk. The correlation intensified with the elapse of time. The changes in the service value of regional ecosystems driven by unreasonable land use will have a great impact on the ecoenvironment. By clarifying the spatiotemporal relationship between ESV and ERI, this research provides theoretical basis and data support to the formulation of ecoenvironmental restoration and protection plans for the upper reaches of the Minjiang River and to the coordinated development between society, economy, and ecoenvironment in the region.

## 1. Introduction

Ecosystem service assessment and ecological risk assessment are closely correlated with each other. Both are important aspects of ecosystem quality assessment [1]. Ecosystem services are the supply of various material products and intangible services obtained by humans from

the ecosystem. The ecological risk mirrors the ecoenvironmental situation and reflects the security of regional ecology [2, 3]. The integration of ecosystem services and ecological risks can effectively introduce ecosystem services into ecological risk assessment, making ecosystem assessment more complete [4]. At present, the research on ecosystem services and that on ecological risks have gradually

moved closer to each other, forming new research hotspots and directions [5].

Land use, the closest bond between human and nature, refers to the way and state of human utilization of the natural features and functions of land [2, 6–10]. Land use changes are an integral part and a major driver of the variation in regional ecoenvironment. It comprehensively reflects the interaction between multiple factors within the terrestrial ecosystem. The continuous change of land use patterns brings changes to the service functions of regional ecosystem [11]. In recent years, many scholars started to study ecoenvironment from the angle of land use. There is a close relationship between land use and ecosystem services. Different types of land use vary significantly in the value of individual ecosystem services. The changes in land use are often resulted from the combined effects of human activities and natural changes, which in turn affect regional ecosystems [12]. The land use pattern affects the living environment and the distribution of resources, as well as the ecosystem service functions. The difference in ecosystem services stems from the disparity in land [13, 14]. Costanza et al. [15] were the first to determine the calculation theory and method of ecosystem service value (ESV). Xie et al. [14, 16] proposed the ESV equivalence system in the light of the actual situation of China and constructed a dynamic evaluation system for China's territorial ecosystem values based on the value equivalent factor per unit area method. Since then, the ESV theory has been continuously applied to assess the ecosystem service capabilities of watersheds, farmlands, cities, wetlands, etc. [17–20]

With the deepening of research, the ecosystem risk caused by land use changes has piqued more and more interests. The land cover variation induced by land use change alters the structure and function of the ecosystem, which in turn influence a series of ecological processes, such as the air, soil, water cycle, and biology [21]. Land use changes, especially land degradation, will bring a string of ecological risks and worsen ecosystem services. Therefore, how to quantify the ecological risk brought by land use has become the focus of research. Relevant research methods include the relative risk model (RRM) [22], the  $R = P \times D$  model, and the ecological risk index (ERI) [23]. Many algorithms are emerging in the meantime, such as genetic algorithm, ant colony algorithm, and particle swarm optimization [24]. On this basis, multiple evaluation frameworks have been established for the ecological risk under land use changes, namely, the pressure-state-response (PSR) framework, the risk probability-sensitivity-intensity (PSI) framework, the driver-pressure-state-response (DPSR) framework, and the driver-pressure-state-impact-response (DPSIR) framework. These frameworks were utilized to quantify the land use ecological risk in different regions [25–27].

The above analysis shows that land use variation affects the ESV. Irrational use of land will bring ecological risks of different degrees. The relationship between ecosystem and ecological risk under land use changes has always been a key research problem. However, few scholars have investigated the mountain-plain transition zones, which are fragile ecologically and prone to mountain disasters. The upper

reaches of the Minjiang River, a typical mountain-plain transition zone in China, serve as a key ecological barrier of the Chengdu Plain, and directly bear on regional ecological security. According to the existing research results, there is a spatiotemporal correlation between the ESV and ecological risks [1, 4, 5]. Based on this understanding, this paper assumes that the spatiotemporal correlation exists in the upper reaches of the Minjiang River and relies on the value equivalent factor per unit area method to quantify the spatiotemporal evolution of ESV and ERI in the study area, using the data on land use. On this basis, the spatial relationship between ESV and ERI was investigated in details. The research results clarify the ecosystem quality of the upper reaches of the Minjiang River from both ESV and ERI, help to grasp the spatiotemporal relationship between ESV and ERI, provide basic data support to the coordinated promotion of the ecosystem service improvement and comprehensive management of the ecoenvironment in the upper reaches of the Minjiang River, and promote the synergistic development between society, economy, and ecoenvironment in the region.

## 2. Materials and Methods

*2.1. Study Area.* The upper reaches of the Minjiang River belong to the eastern margin of the Qinghai-Tibet Plateau (30.7°N–33.2°N, 102.5°E–104.3°E) (Figure 1). With a drainage area of about 24,783.08 km<sup>2</sup>, this region has a great significance ecologically, for it is the primary ecological barrier and water source of the Chengdu Plain. The terrain of the region is high in the northwest and low in the southeast. The mean elevation surpasses 3,000 m. The region is crisscrossed by river valleys with a height difference of more than 5,000 m. There is a huge elevation difference (2,000–3,000 m) between the ridges and river valleys. The study area has various types of landforms, ranging from plateaus to high mountains. Strong tectonic movements have brought frequent geological disasters to the region. Extremely serious mountain geological disasters have hit the region, namely, the Wenchuan earthquake, and the Maoxian County high landslide. In addition, the ecoenvironment is fragile, and soil erosion is serious. As a plateau alpine monsoon climate zone, the study area features vertically distributed climate belts, as well as cold winters and cool summers. The soil types are mainly alpine meadow soil, brown soil, yellow-brown soil, and cinnamon soil; the vegetation types are mainly coniferous forest, shrub, alpine meadow, subalpine coniferous forest, and dry valley shrub.

*2.2. Research Data.* The land use data come from the Resource and Environment Science and Data Center (<http://www.resdc.cn>), and its spatial resolution is 30 m × 30 m. Using ArcGIS, the land use types were classified into six categories: farmland, forestland, grassland, water area, construction land, and unused land. The main information source is the remote sensing images shot by Landsat satellites. The data of 2000, 2005, and 2010 were taken from the remote sensing images of Landsat-TM/ETM. The data of 2015 and 2020 were taken from those of Landsat 8. The

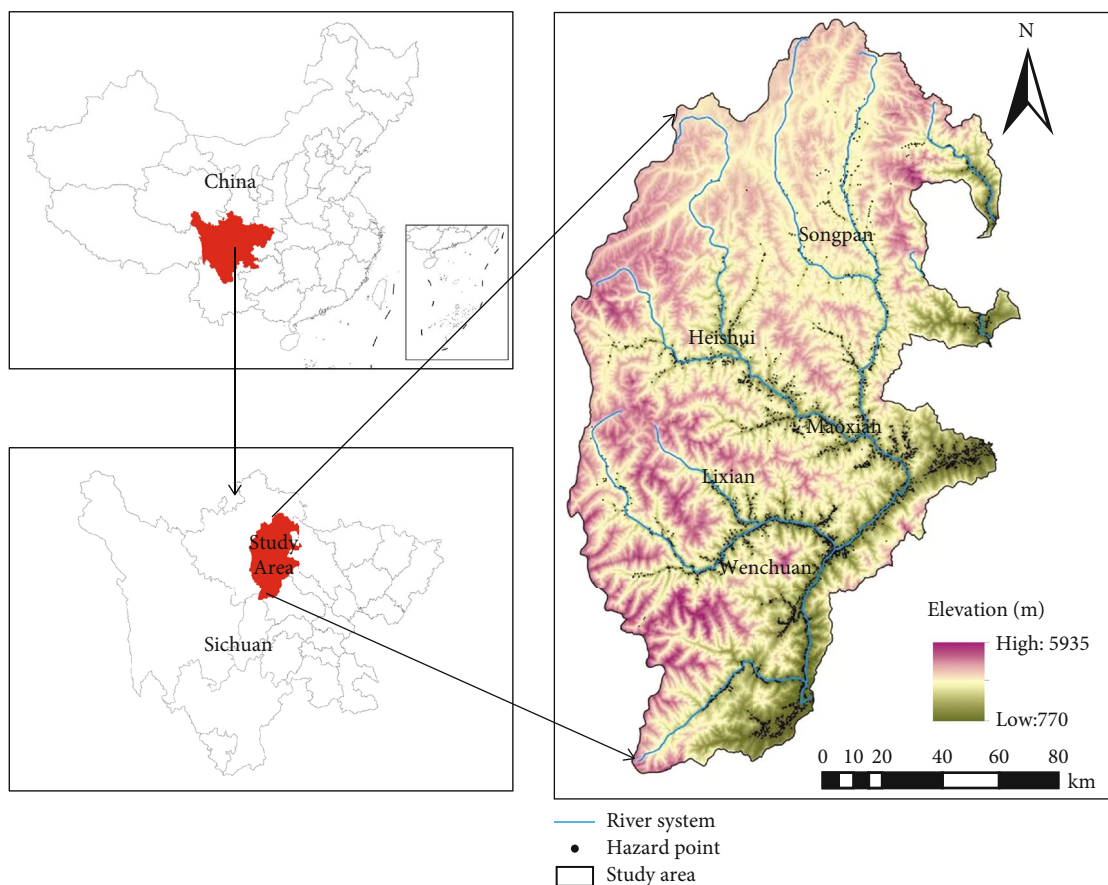


FIGURE 1: Location of study area.

highly precise data guarantee the reliability of the calculated ESV values in the subsequent analysis. The DEM data were obtained from SRTM (Shuttle Radar Topography Mission) of Resources and Environmental Science and Data Center, with a spatial resolution of  $30 \times 30$  m, an absolute horizontal accuracy  $\pm 20$  m, and an absolute elevation accuracy  $\pm 16$  m. The elevation and slope were extracted from the downloaded DEM. The socioeconomic data, namely, crop yield per unit area and sown area of crops, are mainly gathered from *China Statistical Yearbooks* and *Sichuan Provincial Statistical Yearbooks*. The food prices were obtained from <http://www.scgrain.com/>.

**2.3. Methods. ESV.** Ecosystem services refer to the life support products and services obtained directly or indirectly through the structure, process, and function of the ecosystem, which are usually evaluated by market valuation and consumer willingness to pay [5]. Costanza et al. divided the global ecosystem services into 17 different types of services and 16 biomes and calculated the global annual ESV, making the quantitative assessment of ESV a research hot topic. This method has been widely to evaluate the value of various ecosystem services [15]. However, their analysis is unfolded on the global scale. If their method is directly adopted, the ESV of the study area in this research will be estimated with large deviations.

Taking the situation in China as the baseline, Xie et al. [14] formulated the following calculation model of economic value, in reference to Costanza’s research and the studies of ecological scholars in China [14, 16]:

$$VC_k = 1/7 \sum_{i=1}^n \frac{m_i P_i q_i}{M}, i = (1, 2 \dots \dots n), \quad (1)$$

where  $VC_k$  is the economic value of the food production function provided by a unit area of farmland ecosystem ( $\text{yuan}/\text{hm}^2$ );  $i$  is the type of crop;  $P_i$  is the man price of type  $i$  crop ( $\text{yuan}/\text{kg}$ );  $q_i$  is the per unit area yield of type  $i$  crop ( $\text{kg}/\text{hm}^2$ );  $m_i$  is the sown area of type  $i$  crop ( $\text{hm}^2$ );  $M$  is the total sown area of all grain crops.

The ESV in the upper reaches of the Minjiang River can be calculated by:

$$ESV = \sum (A_k \times VC_k), \quad (2)$$

where  $ESV$  is the total value of ecological services;  $A_k$  is the area of the  $k$ th type of land use.

To eliminate the ESV gap of different types of land use between the study area and China, this paper extracts slope and elevation from the DEM data on the upper reaches of the Minjiang River. Drawing on the socioeconomic data like grain yield per unit area and crop sown area, the economic

TABLE 1: Ecological value coefficients of various land use types in the upper reaches of the Minjiang River (yuan/hm<sup>2</sup>).

| Primary type        | Secondary type                 | Farmland | Forest land | Grassland | Water area | Construction land | Unused land |
|---------------------|--------------------------------|----------|-------------|-----------|------------|-------------------|-------------|
| Supply services     | Food production                | 1109.63  | 404.69      | 130.55    | 1044.36    | 0.00              | 0.00        |
|                     | Raw material production        | 522.18   | 926.87      | 182.76    | 300.25     | 0.00              | 0.00        |
|                     | Water conservation             | 26.11    | 483.02      | 104.44    | 10822.18   | 0.00              | 104.85      |
| Regulation services | Air regulation                 | 874.65   | 3067.81     | 665.78    | 1005.20    | 0.00              | 33.88       |
|                     | Climate regulation             | 469.96   | 9177.31     | 1749.30   | 2989.48    | 0.00              | 26.21       |
|                     | Waste disposal                 | 130.55   | 2597.85     | 574.40    | 7245.25    | 0.00              | 133.46      |
|                     | Hydrological regulation        | 352.47   | 4582.13     | 1279.34   | 133469.21  | 0.00              | 383.80      |
| Support services    | Soil conservation              | 1344.61  | 3733.59     | 809.38    | 1214.07    | 0.00              | 25.14       |
|                     | Nutrient recycling maintenance | 156.65   | 287.20      | 65.27     | 91.38      | 0.00              | 0.00        |
|                     | Biodiversity conservation      | 169.71   | 3394.17     | 731.05    | 3328.90    | 0.00              | 25.62       |
| Cultural services   | Entertainment culture          | 78.33    | 1488.21     | 326.36    | 2467.30    | 0.00              | 16.94       |

value equivalent factor per unit area of ESV in the upper reaches of the Minjiang River was solved and corrected as 1,305.45 yuan·hm<sup>-2</sup>. On this basis, the authors derived the ESVs per unit area of different lands in the study area (Table 1).

*ERI*. Ecological risk refers the risk that an ecosystem and its components bear under the disturbance of natural or human activities. It refers to the possible adverse effects of uncertain accidents or disasters on the structure and function of ecosystems in a certain area. Numerous studies have shown a close correlation between land use change and ecological risk and considered land use change the greatest impactor of the ecosystem [5]. Using the area ratio of each land type, the authors constructed the *ERI* and built the empirical relationship between land use structure and regional ecological risk. The relationship was used to measure the relative magnitude of ecological risk in grid units [23]. The *ERI* can be calculated by:

$$ERI = \sum_{i=1}^N \frac{A_{ki}}{A_k} W_i, \quad (3)$$

where *ERI* is the ecological risk index;  $A_k$  is the total area of the  $k$ th sample plot;  $A_{ki}$  is the total area of type  $i$  land in the  $k$ th sample plot;  $W_i$  is the ecological risk intensity of type  $i$  land;  $N$  is the number of types of land use.

Comparing different grid sizes, it was found that a large grid size would sacrifice the coupling effect, and a small grid size would result in data redundancy. Finally, 1 km × 1 km was chosen as the optimal grid size. This paper sets the grid size to 1 km × 1 km, with a total of 24,927 grids. The *ERI* of each type of land use was determined through literature review, in consultation with experts on land management and ecological risk evaluation [28]. The mean *ERI* of each grid was solved. Through analytical hierarchy process (AHP), the ecological risk intensity  $W_i$  of different types of land use was solved: forest land 0.0427, farmland 0.1916, construction land 0.3934, water area 0.1425, grassland 0.0726, and unused land 0.1572 [28].

*Coupling Coordination Degree (CCD) Model*. The CCD model reflects the interplay and action mechanism, and coordination state among the systems in the study area. It is widely used in ecoenvironmental research. This paper adopts the CCD model to measure the coupling coordination relationship between the *ESV* and *ERI* in the upper reaches of the Minjiang River [27, 28]. The CCD can be calculated by:

$$C = \frac{ESV_i^k \times ERI_i^k}{(\alpha ESV_i + \beta ERI_i)^{2k}}, \quad (4)$$

$$D = \sqrt{C \times T}, \quad (5)$$

$$T = \sqrt{\alpha ESV_i \times \beta ERI_i}, \quad (6)$$

where  $C$  is the coupling degree index;  $D$  is the CCD index;  $T$  is the composite evaluation index of the two factors;  $ERI_i$  is the normalized *ERI* of the  $i$ th year;  $ESV_i$  is the normalized *ESV* of the  $i$ th year;  $\alpha$  and  $\beta$  are coefficients to be determined. Here,  $\alpha = \beta = 0.5$ .

Exploratory Spatial Analysis (ESA). The spatial relationship between *ESV* and *ERI* in the upper reaches of the Minjiang River can be judged by the global spatial autocorrelation index [29]:

$$EBI = \frac{m}{\sum_{i=1}^m \sum_{j=1}^m} \frac{\sum_{i=1}^m \sum_{j=1}^m \omega_{ij} R_i R_j}{\sum_{i=1}^m (R_i - \bar{R})^2}. \quad (7)$$

The *EBI* reflects whether the spatial values of the object are similar in space. If  $EBI = 0$ , the two values are randomly distributed. In formula (7),  $\omega_{ij}$  is the spatial weight;  $R$  is the mean attribute value;  $R_i$  and  $R_j$  are the mean of factors  $i$  and  $j$ , respectively;  $n$  is the number of units. If  $|Z| > 1.96$ , the correlation is significant.

As a decomposed form of Moran's  $I$ , the local spatial autocorrelation reflects the internal correlation within the study area. The Moran's  $I$  index was corrected by

TABLE 2: ESVs in 2000–2020.

| Time (year) | Statistical type          | Farmland | Forest land | Grassland | Water area | Construction land | Unused land | Sum      |
|-------------|---------------------------|----------|-------------|-----------|------------|-------------------|-------------|----------|
| 2000        | Value ( $10^8$ yuan/year) | 3.5264   | 339.2511    | 84.6721   | 6.5496     | 0.0000            | 0.0081      | 434.0073 |
|             | Proportion (%)            | 0.8125   | 78.1671     | 19.5094   | 1.5091     | 0.0000            | 0.0019      | 100      |
| 2005        | Value ( $10^8$ yuan/year) | 3.5135   | 338.8580    | 84.7706   | 6.5965     | 0.0000            | 0.0081      | 433.7467 |
|             | Proportion (%)            | 0.8100   | 78.1235     | 19.5438   | 1.5208     | 0.0000            | 0.0019      | 100      |
| 2010        | Value ( $10^8$ yuan/year) | 3.6680   | 350.5846    | 81.1639   | 19.5797    | 0.0000            | 0.0233      | 455.0195 |
|             | Proportion (%)            | 0.8061   | 77.0482     | 17.8374   | 4.2030     | 0.0000            | 0.0051      | 100      |
| 2015        | Value ( $10^8$ yuan/year) | 3.6336   | 350.4870    | 81.1593   | 19.3758    | 0.0000            | 0.0233      | 454.6789 |
|             | Proportion (%)            | 0.7992   | 77.0845     | 17.8498   | 4.2614     | 0.0000            | 0.0051      | 100      |
| 2020        | Value ( $10^8$ yuan/year) | 3.6332   | 350.0814    | 81.1945   | 20.7425    | 0.0000            | 0.0235      | 455.6751 |
|             | Proportion (%)            | 0.7973   | 76.8270     | 17.8185   | 4.5520     | 0.0000            | 0.0052      | 100      |

empirical Bayesian method to obtain the corrected local autocorrelation index EBI:

$$EBI_i = \left( R_i \sqrt{V_i} \sum_{j=1}^m \omega_{ij} \left( R_{ij} \sqrt{V_i} \right) \right). \quad (8)$$

### 3. Results

**3.1. Spatiotemporal Evolution Features.** The ESVs in the upper reaches of the Minjiang River in 1995–2020 were solved by formula (1), in reference to Table 1. The results are shown in Table 2.

As shown in Table 2, the total ESV of the study area was  $4.34 \times 10^{10}$  yuan,  $4.33 \times 10^{10}$  yuan,  $4.55 \times 10^{10}$  yuan,  $4.55 \times 10^{10}$  yuan, and  $4.56 \times 10^{10}$  yuan, respectively, in 2000, 2005, 2010, 2015, and 2020. The total value firstly decreased and then gradually increased, but the overall variation was small. The annual mean increase was merely  $1.08 \times 10^8$  yuan. This is consistent with the conclusion of Xiang et al. [29].

Throughout the research period, the ESV proportion of each land use changed, but the changes did not affect the basic structure of ESV. The proportion of forest land in ESV was always more than 75% in the 25 years. The other types of land had a much smaller ESV than forest land. Hence, forest land is the dominant landscape in the upper reaches of the Minjiang River. Grassland is distributed more widely than any other type of land. However, the ESV per unit area of grassland was far smaller than that of forest land. That is why grassland ranked the second in ESV proportion throughout the study period.

In terms of the spatiotemporal variation in ESV, the ESV of the study area reduced by  $2.61 \times 10^7$  yuan from 2000 to 2005. The main reason is the decline in the total ESV of forest land. Grassland was the land type with the largest ESV increment ( $5.72 \times 10^4$  yuan), while forest land was the land type with the largest ESV decrement ( $5.31 \times 10^6$  yuan).

From 2005 to 2010, the ESV of the study area saw a net growth of  $2.13 \times 10^9$  yuan, up by 4.9% from the previous period. The main contributor is the ESV growth (196.82%) of the water area. In this period, forest land also witnessed

a rapid growth of total ESV. Both water area and forest land promoted the rapid growth of ESV.

From 2010 to 2020, the ESV of the study area increased rather slowly, up by only 0.14%, with a net increase of  $6.56 \times 10^5$  yuan. In this period, the water area's ESV continued to increase, realizing a net growth of  $1.16 \times 10^6$  yuan. On the contrary, the ESV of forest land dropped sharply by  $5.03 \times 10^5$  yuan.

Although the uncontrolled expansion of farmland was controlled by the grain for green policy, the high ESV forest land shrunk in the period, owing to the complex topography and frequent disasters in the Minjiang River Basin. As a result, the ESV growth driven by the water area was offset by the ESV loss of forest land. Overall, the total ESV of the study area did not change much in the period. These results suggest that the relevant policies in the upper reaches of the Minjiang River benefit ESV increase, but the rapid loss of ESV in local areas calls for more attention.

**3.2. Spatiotemporal Evolution Features of ERI.** The stable model was used to perform ordinary kriging interpolation on the ecological risk values of 24,927 sample areas in the upper reaches of the Minjiang River during the study period, and the ERI was divided into strongly high ecological risk ( $\geq 0.20$ ), slightly high ecological risk (0.15–0.20), medium ecological risk (0.10–0.15), slightly low ecological risk (0.05–0.10), and strongly low ecological risk ( $< 0.05$ ). The area of each level was counted by the spatial analysis tool of ArcGIS10.2. The results are shown in Figure 2.

As shown in Figure 2(a), there was a certain difference in the spatial distribution of ERI in the upper reaches of the Minjiang River from 2000 to 2020, but the overall change was not large. Most of the areas were strongly low and slightly low ecological risk areas. The strongly low ecological risk areas were relatively concentrated, while the strongly high and slightly high ecological risk areas were scattered and not connected. On the spatiotemporal variation of ecological risk, the trend of 2000–2005 is dominated by the change of strongly low-risk areas in the center of the study area, that of 2005–2010 is dominated by the change of strongly high risk areas in the north and south of the

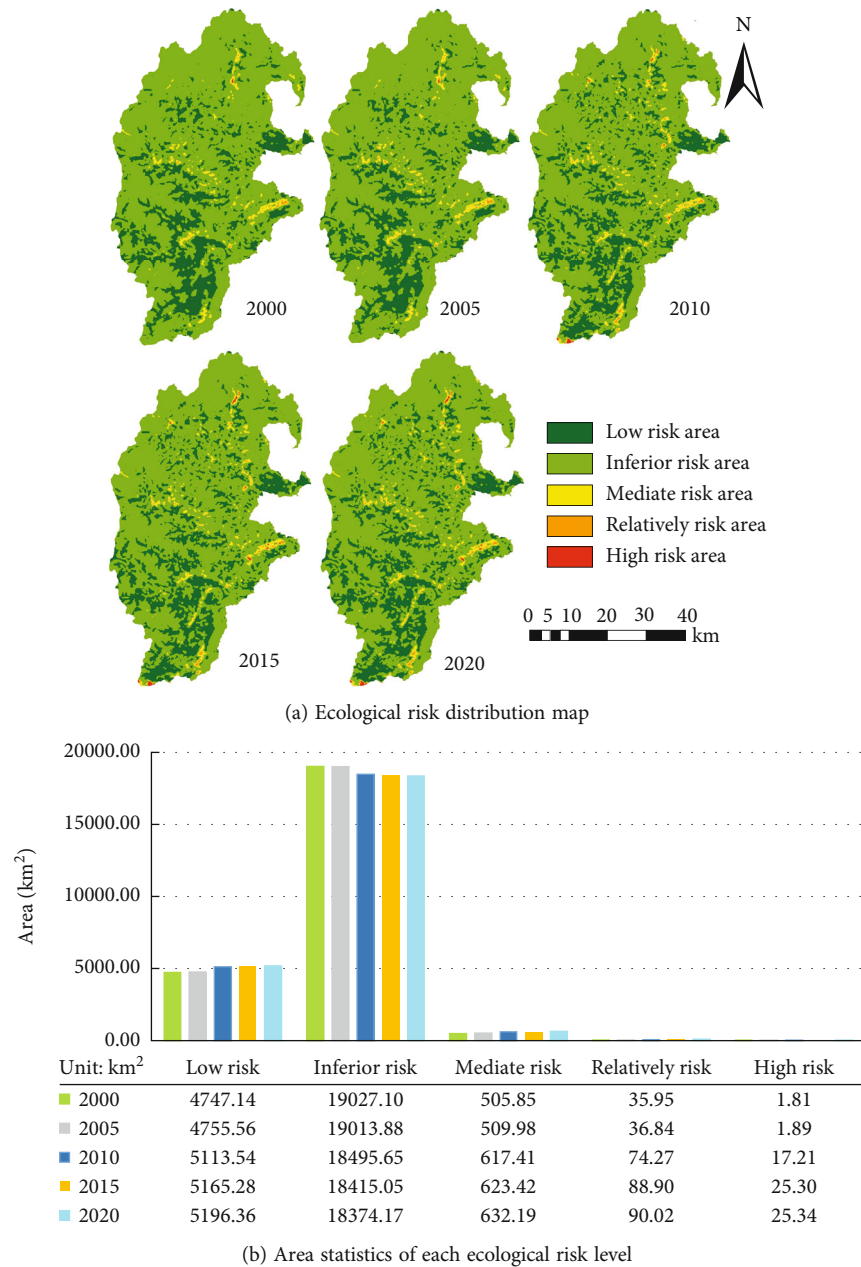


FIGURE 2: Spatiotemporal distribution of ecological risks and the area statistics of each ecological risk level.

study area, and that of 2010–2020 is not significant. The slightly high and strongly high risk areas were located in Chuanzhusi Town and Jin’an Town in the north; Luhua Town, Weigu Township, and Seergu Town in the middle; Shunfu Township and Weimen Township in the east; and Xuankou Town and Sanjiang Town in the south. The strongly low ecological risk areas were relatively concentrated, mainly in Gengda Town, Caopo Township, Putou Town, and Puxi Township in the south, and Baiyang Township in the central and eastern part of the basin. The northern and southern margins of the study area were the main distribution areas of slightly low ecological risk areas, mainly involving Chuanzhusi Town, Caoyuan Town-

ship, Minjiang Township, Yanyun Township, Yinxing Township, and Wolong Town.

As can be seen from Figure 2(b), it should be noted that from 2000 to 2020, although the strongly low and slightly low ecological risk areas dominated the study area, the slightly low ecological risk areas decreased from 19027.1 to 18374.1 km<sup>2</sup>. Meanwhile, the slightly high and strongly high risk areas in 2020 were 2.5 times and 14 times that in 2000, respectively. Overall, there was a continuous growth of ecological risks in local areas.

3.3. *Spatial Relationship between ESV and ERI.* The spatial coupling index between ESV and ERI was calculated by

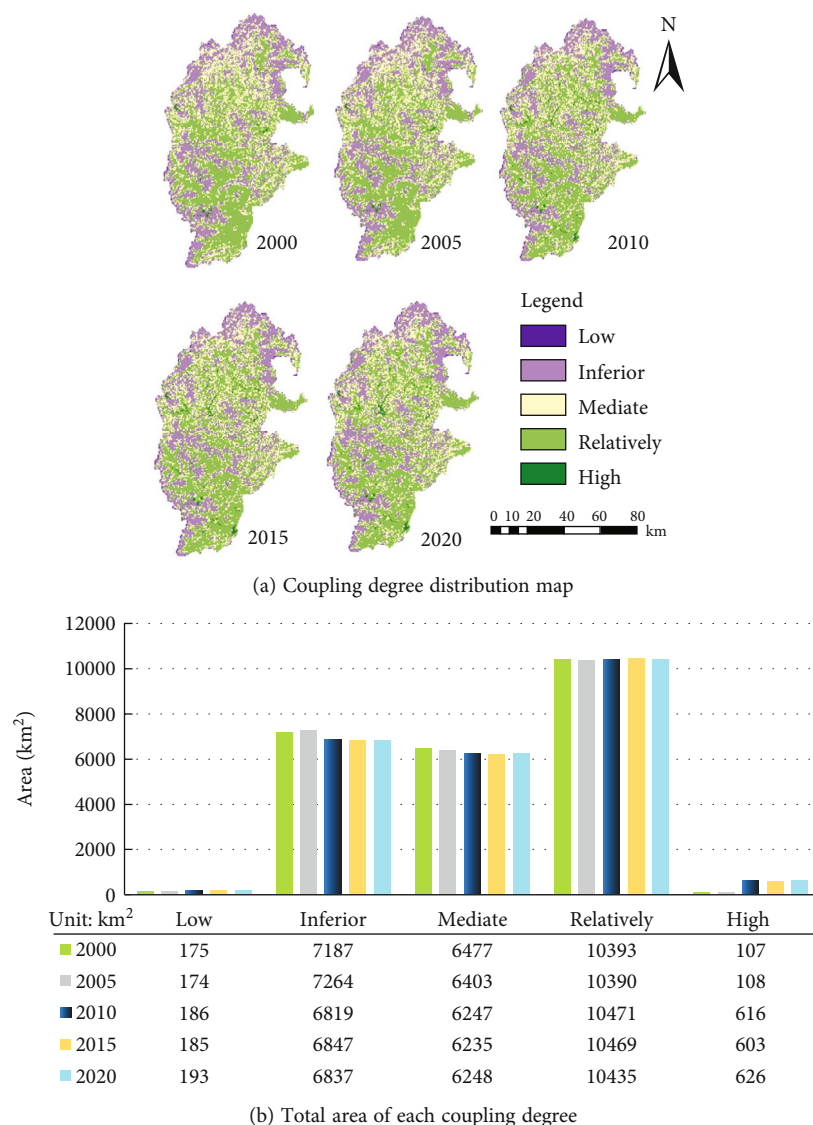


FIGURE 3: Coupling relationship between ESV and ERI and total area of each coupling degree.

formula (4). Then, the coupling degree of each year was divided into five levels by the natural breakpoint method. The total area of each coupling degree was summarized by ArcGIS 10.2 (Figure 3).

As shown in Figure 3(a), the coupling degree of ESV and ERI in the upper reaches of the Minjiang River exhibited an obvious spatial differentiation, and the overall coupling degree was low in the north and high in the south. The areas with slightly high coupling degree were the most widely distributed. Such areas were mainly distributed like patches in the river valleys in Wenchuan County and Lixian County and scattered in other places. The slightly low coupling degree was mainly observed in the high-altitude areas; the medium coupling degree was mostly detected along the margins of the areas of strongly high coupling degree. In addition, the strongly high and strongly low coupling degrees were sporadically distributed.

As shown in Figure 3(b), the areas with strongly low or strongly high coupling degree occupied a very small portion

of the study area. In the study period, however, both types of areas exhibited a growing trend. The areas of strongly low coupling degree expanded from 171 to 193 km<sup>2</sup>, while those of strongly high coupling degree increased by nearly six times, from 105 to 626 km<sup>2</sup>.

In general, the areas with slightly low, medium, and slightly high coupling degrees shrunk slightly in the study period. The areas with slightly high coupling degree boasted the highest proportion (43%), while the proportions of the areas with slightly low coupling degree and those with medium coupling degree did not change much, which remained at around 29% and 26%, respectively. Judging by the coupling between ERI and ESV, the high ESV areas are coupled closely with the low ERI areas, indicating the spatial correlation between ESV and ecological risk.

Further analysis of the CCD between ESV and ERI in the study area (Figure 4) shows that ERI and ESV were in coordinated development in most areas, but large stretches of uncoordinated development were observed. From 2000 to

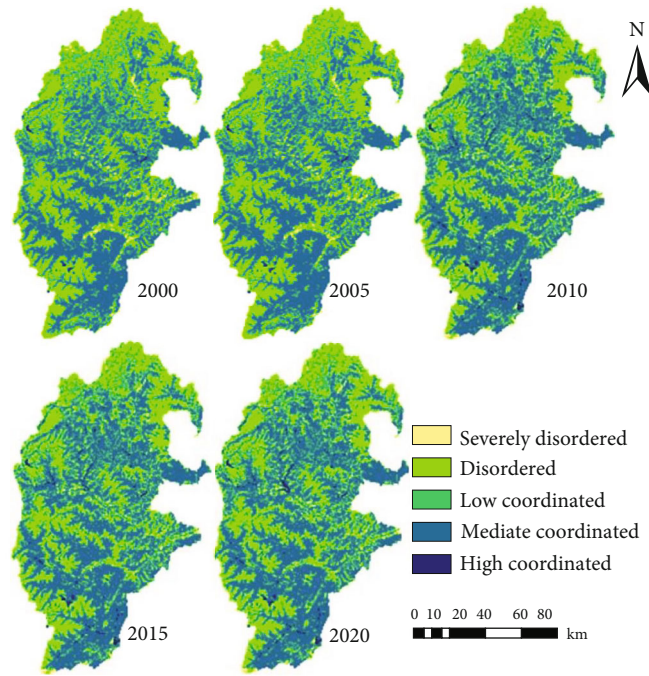


FIGURE 4: CCD between ERI and ESV.

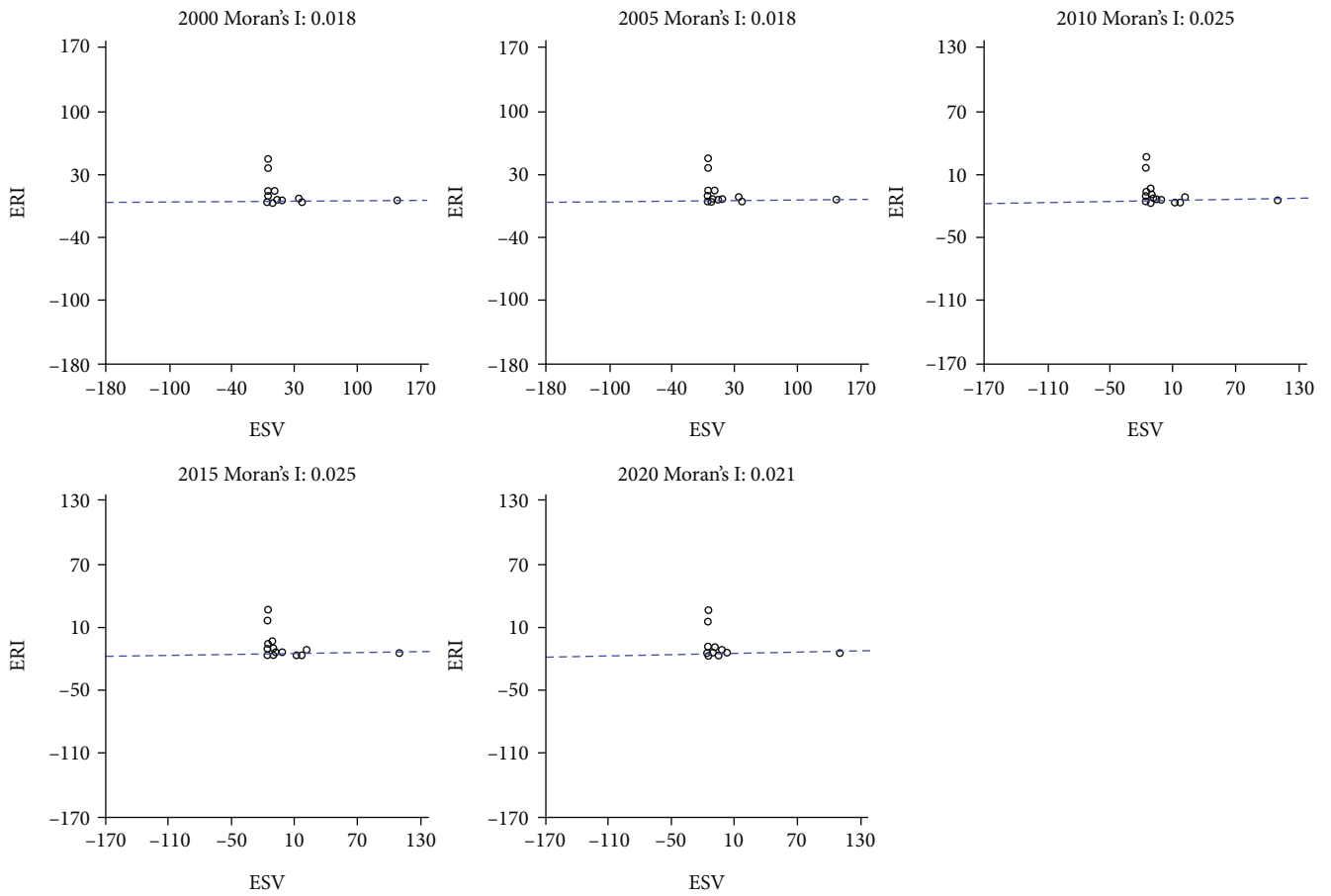


FIGURE 5: Scatterplot of Moran's I.

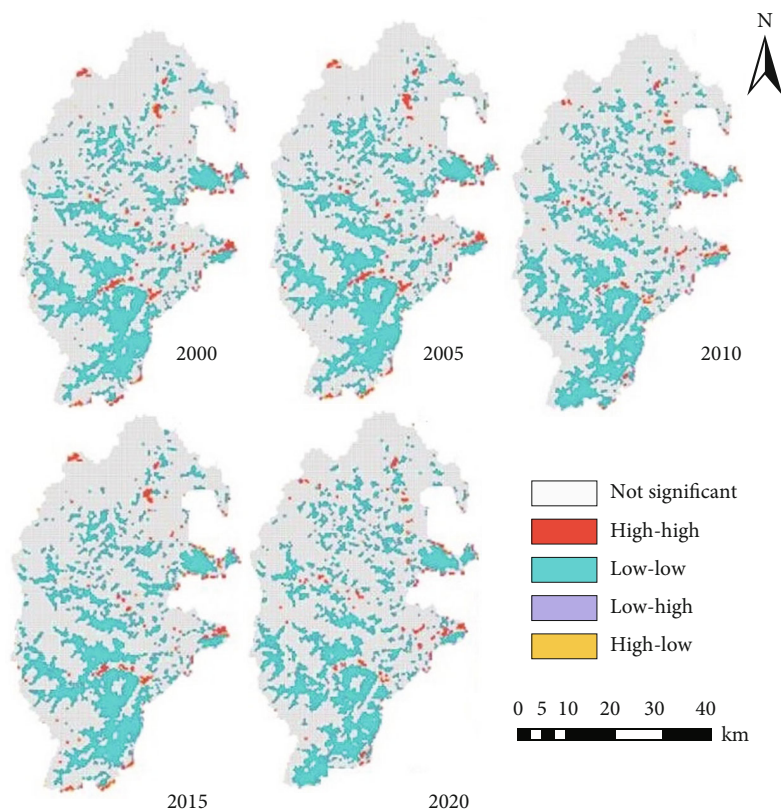


FIGURE 6: Scatterplot of local spatial autocorrelation.

2005, the CCD was high in the middle and south, forming patches in the south, and low and scattered in the north. From 2005 to 2020, the CCD in the north was optimized, and the strongly high coordinated areas increased along river valleys. In terms of the type of coupling coordination, the strongly high coordinated areas occupied a small portion, which increased significantly since 2010. The increase was mainly achieved in river valleys of Heishui County, Lixian County, and Wenchuan County. Many strongly uncoordinated areas existed in scattered form from 2000 to 2015. From 2005 to 2020, the strongly uncoordinated areas were generally on the decline.

Spatial Relationship Analysis Based on Autocorrelation Method. The spatial autocorrelation index between ESV and ERI was calculated by formula (7). The results in Figure 5 show that the Moran's  $I$  between ESV and ERI in the upper reaches of the Minjiang River was 0.018, 0.018, 0.018, 0.025, 0.025, and 0.021, respectively. EBI was always greater than 0, indicating that there was a certain spatial correlation. The overall correlation was not high. The global spatial correlation analysis shows that the spatial distribution of ERI and ESV in the upper reaches of the Minjiang River was not random. There was a certain correlation between ecological risk and ESV, but the relationship was relatively weak. After 2005, the degree of correlation continued to increase. However, the correlation started to weaken in 2020. Therefore, it is necessary to take targeted ecological restoration measures, optimize the ecosystem environment in discrete areas, and continuously enhance the ecosystem service capacity.

Further, the local spatial autocorrelation between ESV and ERI was calculated by formula (8). The results in Figure 6 show that the high-high and low-low cluster areas of ESV and ERI correlation in the study area were basically stable. The high-high cluster areas were scattered in the middle; the low-low areas were mostly concentrated in river valleys; the low-high and high-low areas were rather few. ESV and ERI were uncorrelated in most cases.

When it comes to the time-variation of the spatial correlation between ESV and ERI, after 2005, the high-high areas in the north declined clearly, while those in the south became less concentrated. This trend is closely associated with the grain for green project and mainly affected by human activities. Hence, the high-high areas largely fell to regions with intense human activities.

There were many low-low areas of ESV-ERI correlation, most of which belonged to the south and middle of the study area. A few low-low areas concentrated in the east. Thus, the low ERI areas have a slightly high ESV. The main reason is as follows: this area is mainly an ecological reserve, with a humid and mild climate. After the Wenchuan earthquake, ecological restoration and protection were accelerated, the vegetation coverage was fully restored, and the landscape was no longer fragmented.

#### 4. Conclusions and Discussion

This paper targets the main ecoenvironmental problems in the upper reaches of the Minjiang River, a typical

mountain-plain transition zone in China, and quantifies the spatiotemporal evaluation features of ESV and ERI in the region, using the land use data, and, on this basis, explores the spatial relationship between the two factors. The main conclusions are as follows:

- (1) From 2000 to 2020, the total ESV exhibited a fluctuating upward trend; the areas with a slightly high ESV increased with fluctuations and were distributed relatively concentratedly. In most towns and townships in the study area, the ESV belonged to the slightly low and slightly high levels. The spatial distribution of ESV was greatly affected by slope and altitude, which led to obvious differences in its spatial distribution
- (2) The upper reaches of the Minjiang River had a strongly to slightly low ERI, and a slightly low ERI. The medium, slightly high, and strongly high risk areas took up small proportions in the study area, a sign of relatively good overall ecoenvironment. From 2005 to 2010, the ecological risk changed violently, owing to the Wenchuan earthquake and its secondary disasters. After 2010, slightly high and strongly high risk areas continued to widen. The new slightly high and strongly high risk areas mainly belonged to regions with frequent human activities, such as low altitude areas and river banks
- (3) In the study area, very few regions had strongly low or strongly high coupling degrees between ESV and ERI, but more and more regions witnessed a strongly high coupling degree. The CCD was mainly strongly low, medium, and strongly high and went through violent spatial changes with the elapse of time. There was a certain spatial correlation between ESV and ERI. The low-low cluster feature was very prominent, suggesting that high ESV areas tend to have a slightly low ERI
- (4) The research on the spatiotemporal relationship between ESV and ERI can better link human well-being with the sustainable development of the ecoenvironment and provide decision-making basis for regional ecoenvironmental protection and risk management. This paper focuses on the spatiotemporal relationship between ESV and ERI in the upper reaches of the Minjiang River. However, the changes of regional ESV and ERI are the combined results of multiple factors. Admittedly, this study focuses on the temporal and spatial relationship between ESV and ERI. Yet it fails to fully reflect the relationship and influence the mechanism and evolution trend of these two factors. To make up for the gap, the future research will build a more precise and applicable evaluation system, comprehensively evaluate regional ESV and ERI changes under the combined influence of multiple factors, provide inspiration for IPBES global ecosystem service assessment and

IPCC AR6, and contribute more to the control of global warming

## Data Availability

The data used to support the findings of this study are available from the corresponding author upon request.

## Conflicts of Interest

The authors declare that they have no conflicts of interest.

## Acknowledgments

This research was supported by the Sichuan Science and Technology Program (2022NSFSC1096).

## References

- [1] Y. Y. Jia, X. L. Tang, and W. Liu, "Spatial-temporal evolution and correlation analysis of ecosystem service value and landscape ecological risk in Wuhu City," *Sustainability*, vol. 12, no. 7, p. 2803, 2020.
- [2] B. J. Fu and L. W. Zhang, "Land-use change and ecosystem services: concepts, methods and progress," *Progress in Geography*, vol. 33, no. 4, pp. 441–446, 2014.
- [3] G. J. Piet, A. M. Knights, R. H. Jongbloed, J. E. Tamis, P. de Vies, and L. A. Robinson, "Ecological risk assessments to guide decision-making: methodology matters," *Environmental Science & Policy*, vol. 68, pp. 1–9, 2017.
- [4] Y. Perrodin, C. Boillot, R. Angerville, G. Donguy, and E. Emmanuel, "Ecological risk assessment of urban and industrial systems: a review," *Science of the Total Environment*, vol. 409, no. 24, pp. 5162–5176, 2011.
- [5] J. H. Li and M. X. Gao, "Spatiotemporal evolution and correlation analysis of ecosystem service values and ecological risk in Bizhou," *Acta Ecologica Sinica*, vol. 39, no. 21, pp. 7815–7828, 2019.
- [6] J. Zhang, Q. Q. Li, X. Y. Wu, C. C. Zhang, J. Z. Wang, and G. F. Wu, "Evolution of the ecosystem services value and carrying capacity in the Guangdong-Hong Kong-Macao Greater Bay Area based on land use changes," *Acta Ecologica Sinica*, vol. 41, no. 21, pp. 1–12, 2021.
- [7] M. Mujiyo, I. F. Suprpto, A. Herawati et al., "Land suitability assessment for cassava var. Jarak Towo, using determinant factors as the strategy fundament in hilly area Jatiyoso-Indonesia," *International Journal of Sustainable Development and Planning*, vol. 16, no. 6, pp. 1131–1140, 2021.
- [8] H. Q. Wang and S. Cheng, "Spatiotemporal variation in land use of Northeast China Tiger and Leopard National Park," *International Journal of Design & Nature and Ecodynamics*, vol. 15, no. 6, pp. 835–842, 2020.
- [9] D. O. Onyango, C. O. Ikorukpo, J. O. Taiwo, and S. B. Opiyo, "Land use and land cover change as an indicator of watershed urban development in the Kenyan Lake Victoria Basin," *International Journal of Sustainable Development and Planning*, vol. 16, no. 2, pp. 335–345, 2021.
- [10] N. Naharuddin, A. Malik, I. Rachman, H. Muis, H. Hamzari, and A. Wahid, "Land use planning for post-disaster soil liquefaction area based on erosion hazard index," *International Journal of Design & Nature and Ecodynamics*, vol. 15, no. 4, pp. 573–578, 2020.

- [11] M. Xiang, J. Yang, W. Li et al., "Spatiotemporal evolution and simulation prediction of ecosystem service function in the western Sichuan plateau based on land use changes," *Frontiers in Environmental Science*, vol. 10, p. 890580, 2022.
- [12] B. Shrestha, Q. Ye, and N. Khadka, "Assessment of ecosystem services value based on land use and land cover changes in the transboundary Karnali River basin, Central Himalayas," *Sustainability*, vol. 11, no. 11, p. 3183, 2019.
- [13] B. Fu, S. Wang, C. Su, and M. Forsius, "Linking ecosystem processes and ecosystem services," *Current Opinion in Environmental Sustainability*, vol. 5, no. 1, pp. 4–10, 2013.
- [14] G. D. Xie, C. X. Lu, Y. F. Leng, D. Zheng, and S. C. Li, "Evaluation of ecological assets in Qinghai-Tibet Plateau," *Journal of Natural Resources*, vol. 18, no. 2, pp. 189–196, 2003.
- [15] R. Costanza, R. d'Arge, R. De Groot et al., "The value of the world's ecosystem services and natural capital," *Nature*, vol. 387, no. 6630, pp. 253–260, 1997.
- [16] G. D. Xie, C. X. Zhang, L. M. Zhang, W. H. Chen, and S. M. Li, "Improvement of the evaluation method for ecosystem service value based on per unit area," *Journal of Natural Resources*, vol. 30, no. 8, p. 1243, 2015.
- [17] J. Zhou, J. Wu, and Y. Gong, "Valuing wetland ecosystem services based on benefit transfer: a meta-analysis of China wetland studies," *Journal of Cleaner Production*, vol. 276, p. 122988, 2020.
- [18] H. Temesgen, W. Wu, X. Shi, E. Yirsaw, B. Bekele, and M. Kindu, "Variation in ecosystem service values in an agroforestry dominated landscape in Ethiopia: implications for land use and conservation policy," *Sustainability*, vol. 10, no. 4, p. 1126, 2018.
- [19] X. Dai, B. A. Johnson, P. Luo et al., "Estimation of urban ecosystem services value: a case study of Chengdu, southwestern China," *Remote Sensing*, vol. 13, no. 2, p. 207, 2021.
- [20] F. P. Fang, J. F. Feng, F. B. Li, and S. B. Peng, "Impacts of the north migration of China's rice production on its ecosystem service value during the last three decades (1980-2014)," *Journal of Integrative Agriculture*, vol. 16, no. 1, pp. 76–84, 2017.
- [21] J. Wang, W. Bai, and G. Tian, "A review on ecological risk assessment of land use," *Journal of Natural Resources*, vol. 35, no. 3, pp. 576–585, 2020.
- [22] W. G. Landis and J. A. Wieggers, "Design considerations and a suggested approach for regional and comparative ecological risk assessment," *Human and Ecological Risk Assessment*, vol. 3, no. 3, pp. 287–297, 1997.
- [23] P. Tian, J. Li, H. Gong et al., "Research on land use changes and ecological risk assessment in Yongjiang River Basin in Zhejiang Province, China," *Sustainability*, vol. 11, no. 10, p. 2817, 2019.
- [24] Y. Nie, N. Li, and C. Hu, "Enhanced inhibition of bromate formation in catalytic ozonation of organic pollutants over Fe-Al LDH/Al<sub>2</sub>O<sub>3</sub>," *Separation and Purification Technology*, vol. 151, pp. 256–261, 2015.
- [25] Q. G. Zhou, X. Y. Zhang, and Z. L. Wang, "Land use ecological risk evaluation of the Three Gorges Reservoir area in Chongqing based on PSR model," *Research of Soil and Water Conservation*, vol. 20, no. 5, pp. 187–192, 2013.
- [26] D. Liu, H. Chen, Q. Q. Shi, H. Zhang, and T. W. Geng, "Spatio-temporal variation of ecological risk in the loess hilly-gully region and its precaution partitions: a case study of Mizhi county, Shaanxi Province China," *Journal of Natural Resources*, vol. 34, pp. 2012–2025, 2019.
- [27] Z. Wang, J. H. Liu, T. S. Li, Z. Ruan, and F. Q. Wu, "Analysis of the coupling relationship between ecological vulnerability and economic poverty in Qinling-Dabashan contiguous poor areas: a case study of Shanyang County in Shaanxi Province, China," *Acta Ecologica Sinica*, vol. 39, no. 11, pp. 3908–3917, 2019.
- [28] X. Y. Chen, G. Z. Xie, and J. P. Zhang, "Landscape ecological risk assessment of land use changes in the coastal area of Haikou City in the past 30 years," *Acta Ecologica Sinica*, vol. 41, no. 3, pp. 975–986, 2021.
- [29] M. Xiang, L. Duan, F. Wei et al., "Analysis on the spatial differentiation characteristics of poverty risk caused by disaster under the stress of geological disasters: a case study of Sichuan Province," *Environmental Science and Pollution Research*, vol. 29, no. 34, pp. 52111–52122, 2022.